A Piezoresistive MEMS Memory Device Using a Buckled Beam

Jerry A. Yang*, Pranoy Deb Shuvra**, Ji-Tzuoh Lin**, Kevin Walsh**,
Shamus McNamara** and Bruce Alphenaar**

* University of Texas at Austin, Austin, TX, USA, jerryyang747@utexas.edu
** University of Louisville, Louisville, KY, USA, kevin.walsh@louisville.edu

ABSTRACT

Microelectronics and microelectromechanical systems (MEMS) have given rise to a large class of new devices, from ultra-miniature sensors for cell phones and automobiles to complex memory devices for computers. Recent research in memory devices has largely focused on designing new non-volatile forms of electronic memory, yet a MEMS-based memory device has not been proposed in the literature. This work presents a novel MEMS memory device using an asymmetrical, bistable buckled beam. Relying on well-known MEMS structures and the piezoresistive effect, the MEMS memory model was first conceptually designed, then optimized for signal strength using CoventorWare finite-element modeling. In the optimization process, various aspects of the devices geometry were ranked in order of magnitude of influence on the devices output signal strength, then optimized based on their importance. Simulation results indicate that the optimized device can generate signals up to 5.5uV with a supply voltage of 2.5V, a 27.5x improvement over the initial design. The length and width of the beam were found to be the most influential factors in controlling the signal output: increases in beam width lead to significant increases in signal when paired with the corresponding beam lengths. However, large beam widths caused the beam to buckle into higher-order modes when the beam was short, leading to sharp decreases in signal. Other geometric factors had only minor impacts on signal strength. The MEMS memory device paves the way for future low-power, radiation-hard MEMS memory models.

Keywords: MEMS, memory, optimization, modeling

1 INTRODUCTION

As computers become increasingly powerful, innovative memory types and architectures are required to store and process the increasingly complex tasks computers complete. Memory devices must be small and use little power, yet be insensitive to radiation and scalable to industry standards. Recent research in nonvolatile memory has generated numerous unique approaches and designs, from field-effect transistor (FET) devices [1] made from organic materials to flexible all-carbon devices [2]. Other non-volatile memory research has also focused on electrochemical and resistive switches [3]. One field that has not contributed to the plethora of current non-volatile memory devices is microelectromechanical systems (MEMS). The rapid growth of MEMS applications has caused a proliferation of MEMS devices such as pressure sensors, gyroscopes, accelerometers, microfluidic devices, RF devices and more [4] [5]. Yet there have only been a few MEMS memory devices reported in the literature. Reference [6] showcases a MEMS memory design using a suspended gate MOSFET, and [7] describes a cantilever device that uses vibrational deactuation for high-temperature operation. While the MOSFET device in [6] is easily scalable and the cantilever in [7] is robust under extreme temperature conditions, neither device has been shown to be low-power or radiation-hard.

This paper proposes a novel MEMS memory device utilizing a bistable buckled beam. The paper first describes the theoretical development and operation of the model, then proceeds with the models geometric optimization. Several trends discovered in the optimization process are discussed, and limitations of the optimized device model and future directions are considered.

2 DEVICE MODEL

2.1 Development

The first MEMS memory model proposed was a silicon cantilever beam that had a symmetric base relative to the beam axis, first reported in [8]. The state of the memory device would be determined by the piezoresistance of the base when the beam was bent one way or the other. Due to the symmetry of the device, there was a negligible piezoresistance between the two states. To increase the difference in piezoresistance of the device, the base was widened on one side of the beam, creating an asymmetrical base. However, the device was not bistable: without constant actuation, the cantilever would return to its upright (non-bent) position. The current model uses a lateral bistable buckled beam derived from [9]. To ensure that the piezoresistance of the device would be different in both buckled states of the beam, one side of each of the bases was thickened as shown in Fig. 1. Since silicon has a high piezoresistivity

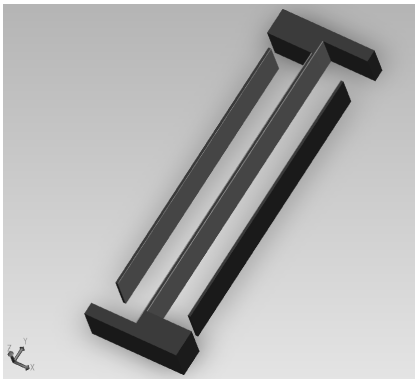

Figure 1: Lateral bistable buckled beam with asymmetrical bases.

and silicon oxide has a compressive stress of about 350 MPa, measurable differences in piezoresistance could be achieved when the released beam was buckled to the left or right [8]. In Fig. 1, two electrodes were placed on either side of the beam for electrostatic actuation.

2.2 Device Operation

To read the device, the device is placed in series with itself rotated by 180° (see Fig. 2). As shown in the top of Fig. 2, this configuration can be modeled by a Wheatstone bridge circuit with the anchors serving as the variable resistances. When a voltage V_{in} is supplied to the circuit, the Wheatstone bridge will generate a voltage output

$$V_{out} = V_{in}\frac{R_2 - R_1}{R_2 + R_1}. \quad (1)$$

This model assumes that the beam resistance is much larger than resistances of the anchors, which may not be true for long and thick beams.

To write to the device, two electrodes are placed on either side of the beam. When a large voltage is applied to the electrode farther from the beam, it will generate enough attractive force to cause the beam to snap toward the electrode (Fig. 2, bottom). When the voltage is removed, the beam relaxes into the resting state closer to the electrode that actuated it. However, if too large a voltage is applied, the beam will make contact with the electrode, potentially causing damage. The voltage required for the beam to snap is denoted the switching voltage V_{sw}, and the voltage required for the beam to snap and make contact with the electrode is denoted the pull-in voltage V_{pullin}.

3 OPTIMIZATION METHODOLOGY

A signal strength of 10uV was desired given a 2.5V supply, a switching voltage of 200V, and a pullin voltage 50V greater than the switching voltage were desired.

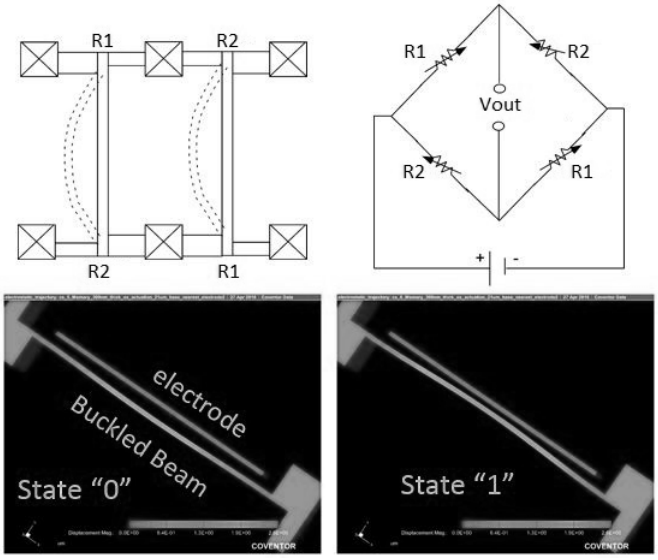

Figure 2: Reading (top) and writing (bottom) to the memory device. Courtesy of Pranoy Deb Shuvra.

To optimize the device, the output parameters were first ranked from most important to least important (see Table 1). Based on the most important output parameter, the input parameters were also ranked (see Fig. 3) from largest effect to smallest effect. One or two input parameters were selected to be optimized at a time, and the optimized model was used to optimize the next set of inputs selected. An initial model geometry was chosen arbitrarily. Table 1 shows the initial parameters, their initial values and their rankings.

Table 1: Initial Parameters and Values, Ranked

Input	**Output**
1. Beam width (1um)	1. Signal strength (0.15uV)
2. Beam length (100um)	2. Switching voltage (60V)
3. Base length (23um)	3. Pull-in voltage (500-600V)
4. Base width ratio (11um : 5um)	4. Beam center displacement (0.48um)
5. Orientation (Si⟨100⟩)	
6. Oxide thickness (350nm)	
7. Electrode distance (2um)	

Simulations were run using CoventorWare 2012. Since the software found the non-buckled state as an equilibrium solution in its mechanical analyses, it was neces-

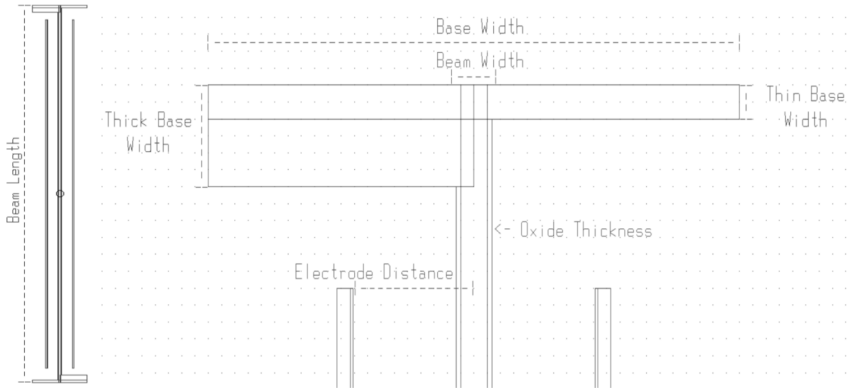

Figure 3: Input parameter definitions.

sary to simulate a force to (bias) the beam and relax it (post-buckle) to find the two stable equilibrium solutions. The currents through the two anchors, reported by CoventorWare for both states in a piezoresistive analysis, were then used to calculate the Wheatstone bridge voltage output for both states, assuming a supply voltage of 2.5V. The voltage difference between the left and right state was then taken as the signal strength. For the switching voltage, the beam was pushed to the right state. Then, a voltage ramp from 0-200V in increments of 10V was applied to the left electrode to cause the beam to buckle into the left state. The minimum voltage required to cause the switch in states was taken as the switching voltage. Similarly, for the pull-in voltage, the beam was pushed to the right state, and a voltage ramp from 200-1000V was applied to the left electrode in a pull-in detection analysis by CoventorWare. The minimum voltage that caused the beam to make contact to the electrode was recorded as the pull-in voltage. Since the switching and pull-in voltage depend on the electrode distance, for these analyses, the electrodes were placed about 2um away from the maximum center deflection reported by the post-buckle analysis.

4 RESULTS

After optimization, the optimized parameters are displayed in Table 2. Though the model does not yield a signal strength greater than 10uV, a signal strength of 5.5uV can be amplified for easier detection (see e.g. [14]). Furthermore, the switching voltage is much smaller than the pull-in voltage, preventing pull-in instability in the write stage. The results for each stage of the optimization process are described below.

Five sets of simulations were run, varying different input parameters in each simulation set. After each simulation set was completed, the best model was used as the initial model in the next simulation set. First, the base length was varied from 5-50um in increments of 5um, and the beam length was varied from 100-200um in increments of 20um and from 200-300um in increments of 50um. A sharp increase in signal occurred as beam lengths increased, peaking in the range of 100-150um before tapering off at larger beam lengths. The best signal was about 0.47uV at base length 40um and beam length 140um, 3x more than the original model.

Table 2: Final Parameters and Values

Input	**Output**
Beam width (2.7um)	Signal strength (5.5uV)
Beam length (320um)	Switching voltage (100V)
Base length (40um)	Pull-in voltage (400V)
Base width ratio (6um : 2um)	Beam center displacement (2.1um)
Orientation (Si⟨100⟩)	Voltage “low” (-4.35uV)
Oxide thickness (350nm)	Voltage “high” (1.15uV)
Electrode distance (9um)	

Second, the beam width was doubled from 1um to 2um. The 2um beam had a signal peak of 0.77uV at base length 40um and beam length 260um, roughly double the signal strength of the previous model. The model also produced voltages of opposite polarities in the left and right state, useful for signal detection. The switching voltage was found to be about 120V, and the pull-in voltage around 400V.

Third, the width of the thin base was tested at 2um, 3um and 5um, while the width of the thick base ranged from 4-15um in in 2um increments. From the data, a less wide thin base led to much higher signal strengths. The base lengths and beam lengths were also re-optimized to ensure the model consistently had the highest signal strength. The model retained its 40um base length and increased the beam length to 320um, which led to a 5.5uV signal strength. Furthermore, the voltage signals produced when the beam was in the left and right state were of similar magnitudes but opposite polarities. The

switching voltage decreased while the pull-in voltage remained the same, suggesting that so long as the beam was sufficiently long enough, the switching and pull-in voltages could be kept constant when the beam width was increased.

Fourth, to simulate different crystalline orientations of silicon, the model was rotated about the z-axis with respect to the origin, giving a different "planar orientation" with respect to the substrate. Due to the rotational symmetry of the device, rotational angles 0°-165° were simulated in 15° increments. Notably, the signal decreased as the model became less orthogonal to the XY-axes, reaching a minimum at the 45 and 135 rotations. The signal did not increase for any angle, suggesting that the ⟨100⟩ orientation yields the greatest signal.

Fifth, the beam length was set at 1000um and the beam width was varied between 4.7um and 9.7um in 1um increments to determine the optimum width and largest signal. Beams wider than 5.7um settled into the second buckling mode instead of the first. Notably, this phenomenon only occurred during the coupled electromechanical analysis used for the switching and pull-in voltages in CoventorWare the phenomenon was not observed in any of the mechanical analyses that were used in the measurement of the signal. The simulations indicated that signals of 35uV or greater could be achieved, but these results are likely unreliable.

5 CONCLUSION

This paper presents a novel MEMS memory device featuring a buckled beam with asymmetrical bases. Based on an optimization of the device, signal strengths of up to 35uV were observed through simulation. However, considering factors such as geometry, size and orientation, the preferred design yielded a signal strength of 5.5uV with sufficient switching voltage and low pull-in instability, a 37x improvement over the originak design. As a non-volatile memory device, the model serves as a low-power, radiation-hard alternative to conventional memory devices.

Acknowledgment

This work is supported by the University of Louisville IMPACT Research Experience for Undergraduates (REU) program, NSF Award No. 1560235. This work was performed at the University of Louisville Micro/Nano Technology Center, which belongs to the NSF NNCI KY Manufacturing and Nano Integration Node, supported by ECCS-1542174. This work is also supported by the Defense Threat Reduction Agency under Grant No. HDTRA1-15-1-0027. We give thanks to Jim Davidson and Michael Alles from Vanderbilt University for their contributions.

REFERENCES

[1] K. Baeg, Y. Noh, J. Ghim, S. Kang, H. Lee, and D. Kim, "Organic non-volatile memory based on pentacene field-effect transistors using a polymeric gate electret," *Adv. Mater.*, vol. 18, pp. 3179-83, Nov. 2006.

[2] J. Liu, Z. Yin, X. Cao, F. Zhao, L. Wang, W. Huang, and H. Zhang, "Fabrication of flexible, all-reduced graphene oxide non-volatile memory devices," *Adv. Mater.*, vol. 25, pp. 233-8, Jan. 2013.

[3] R. Waser, "Resistive non-volatile memory devices," *Micro. Eng.*, vol. 86, pp. 1925-8, July 2009.

[4] J. Bryzek, "Impact of MEMS technology on society," *Sens. Actuators A*, vol. 56, pp. 1-9, Aug. 1996.

[5] V. Kaajakari, *Practical MEMS.* Las Vegas: Small Gear Publishing, 2009.

[6] N. Abele, A. Villaret, A. Gangadharaiah, C. Gabioud., P. Ancey, and A. M. Ionescu, in *Electron Devices Meeting, 2006. IEDM '06. International,* 2006, pp. 1-4.

[7] A. T. Do, J. K. Gopal, P. Singh, G. L. Chua, and T. T. Kim, "A cantilever-based non-volatile memory utilizing vibrational reset for high temperature operation," *IEEE Trans. Electron Devices*, vol 61, pp. 2177-85, June 2014.

[8] P. D. Shuvra, S. McNamara, J. Lin, B. Alphenaar, K. Walsh, and J. Davidson, "Axial asymmetry for improved sensitivity in MEMS piezoresistors," *J. Micromech. Microeng.*, vol. 26, pp. 1-11, July 2016.

[9] M. Vangbo and Y. Backlund, "A lateral symmetrically bistable buckled beam," *J. Micromech. Microeng.*, vol. 8, pp. 29-32, Jan. 1998.

[10] C. S. Smith, "Piezoresistance effect in germanium and silicon," *Phys. Rev.*, vol. 94, pp. 42-9, Apr. 1954.

[11] E. P. EerNisse, "Stress in thermal SiO2 during growth," *Appl. Phys. Lett.*, vol. 35, pp. 8-10, Apr. 1979.

[12] W. C. Young and R. G. Budynas, *Roark's Formulas for Stress and Strain,* 7th ed. New York: McGraw-Hill, 2002, p. 526.

[13] M. Vangbo, "An analytical analysis of a compressed bistable buckled beam," *Sens. Actuators A*, vol. 69. pp. 212-6, Feb. 1998.

[14] B. Radisavljevic, M. B. Whitwick, and A. Kis, "Small-signal amplifier based on single-layer MoS2", *Appl. Phys. Lett.*, vol. 101, 043103, July 2012.